Materials Research Proceedings **16** (2020) 16-26 https://doi.org/10.21741/9781644900710-3

Two Different Acid Oxidation Syntheses to Open C_{60} Fullerene for Heavy Metal Detection

E. Ciotta[1*], L. Burratti[1], P. Prosposito[2], E. Bolli[3], S. Kaciulis[3], S. Antonaroli[4] and R. Pizzoferrato[1]

[1]Department of Industrial Engineering University of Rome Tor Vergata, 00133 Rome, Italy

[2] Department of Industrial Engineering INSTM and CiMER University of Rome Tor Vergata, 00133 Rome, Italy

[3]Institute for the Study of Nanostructured Materials, CNR of Italy, Monterotondo Stazione, 00015 Rome, Italy

[4]Department of Chemical Science and Technologies, University of Rome Tor Vergata, 00133 Rome, Italy

* erica.ciotta@uniroma2.it

Keywords: Carbon Materials, Heavy Metals, Sensors, Spectroscopy, Photoluminescence, Quenching, Chemical Oxidation

Abstract. Graphene oxide quantum dots (GOQDs) can be synthesized through a large variety of synthesis methods starting from different carbon allotropes such as nanotubes, graphite, C_{60} and exploiting various synthesis and reactions. These different approaches have great influence on the properties of the obtained materials, and, consequently, on the potential applications. In this work, Buckminster C_{60} fullerene has been used to prepare unfolded fullerene nanoparticles (UFNPs) via two distinct synthesis methods namely: Hummer and H_2SO_4 + HNO_3 solution. The different characteristics of the final materials and the different response in the presence of heavy metal ions have been investigated in view of sensing applications of water contamination.

Introduction

Graphene oxide quantum dots present unique properties [1] of photoluminescence (PL), biocompatibility, low cytotoxicity and photostability. For all these reasons they have been proposed as candidate material for many applications such as bioimaging and electrochemical biosensor, catalysis, organic light-emitting diodes, and heavy metal detection [2-5]. GOQDs are single or few-layer graphene oxide (GO) sheets with lateral dimensions less than 100 nm [6] exhibiting exciton confinement and quantum-size effect. In a typical structure the presence of oxygen-containing functional groups (–OH, –COOH and epoxy groups) located on the carbon basal plane and at the edges of the sheets are quite common. The consequent large number of sp^3 carbon atoms in the GO lattice opens the optical bandgap of graphene and results in photo-excited fluorescence with a typical, stable blue/green emission which can be exploited for many possible applications [7]. The main role of these groups on the surface, which either form during the synthesis procedures or are intentionally added by specific treatments, consists in improving the hydrophilicity and thus the dispersibility in water. More importantly, they can undergo partial deprotonation in water environment, and this can promote binding of heavy metal cations as substitutes for the lost protons [8,9]. For this reason, GOQDs have been used as sensor of heavy

metals (HMs) ions in water. In fact, chelation of heavy metals has recently been considered as the origin of the fluorescence quenching observed in (GOQDs) [4,10-16]
Although GO is obtained starting from smaller molecules [17] with the so called bottom-up approach, they are usually produced starting from macroscopic materials like graphite, nanotubes, or C_{60} trough a top-down method. The most common synthesis of this type are: acid oxidation [18], electrochemical oxidation [19], hydrothermal [20], microwave radiation [21], chemical exfoliation [22]. In the case of acid oxidation, there are different ways to obtain graphene oxide. In the Staudenmaier method [23], for example, a combination of sulfuric acid and fuming nitric acid and $KClO_3$ are used. In the Hofmann method [24], a combination of sulfuric acid (H_2SO_4), concentrated nitric acid (HNO_3), and potassium chlorate ($KClO_3$) are exploited.

The Hummer method [25], based on a combination of sulfuric acid and $NaNO_3$ and $KMnO_4$ or a mixture between sulfuric acid and nitric acid, represents the most common strategy to obtain GOQDs. This strategy is preferred with respect to other methods due to its higher degree of oxidation [26].

Recently, several groups have applied GOQDs produced in the above mentioned synthesis to the study of the interaction with heavy metal ions.

Different responses were obtained depending on the starting materials, the dimension of GOQDs, the number of functional groups on the edge and on the surface and so on. For example, responses to a number of heavy metal ions have been analyzed starting by exfoliated graphite using modified Hummer method [4,11], or by using pyrolysis of citric acid [12] or chemical oxidation of carbon fibers [16], or Hummer method starting from C_{60} fullerene [27,28]. The results were sometime not comparable and a dependence on synthetic method of production of GOQDs was observed that suggest the need of further studies.

In this work we reported on two different synthesis methods starting from C_{60} fullerene to obtain unfolded fullerene nanoparticles (UFNPs) that are a specific type of GOQDs. The first approach is based on a slight modification of Hummer method, while the second one exploited an acid oxidation synthesis with sulphuric and nitric acid. In both cases, the chemical oxidation of C_{60} caused the opening of the Buckminster structure and the formation of oxygen-containing functional groups, such as –OH and –COOH on the edge and the surface of the structure. Both obtained photoluminescent materials were tested to detect the presence in water of heavy metal ions through the change of its PL intensity. We reported how the optical response depends on the two synthesis methods implemented. Moreover, exploiting X-ray photoemission spectroscopy (XPS) and Fourier Transform Infrared Spectroscopy (FTIR), we analyzed how the observed differences can be related to the morphology and chemical properties of the materials.

Experimental

Materials

C_{60} (Solaris Chem Inc.), sulfuric acid (H_2SO_4, Sigma Aldrich 99.9%), sodium nitrate ($NaNO_3$, Sigma Aldrich), sodium hydroxide (NaOH, Sigma Aldrich), potassium permanganate ($KMnO_4$, Sigma Aldrich), hydrogen peroxide (H_2O_2, Sigma Aldrich), Nitric acid (HNO_3 Sigma Aldrich 99.9%) were used as received without further purification. Deionized water obtained from a Milli-Q water purification system (Millipore) was used for all the synthesis and the sensing test measurements.

Hummer Synthesis (Synthesis A)

In the case of Hummer synthesis, hereafter referred to as synthesis A, UFNPs were prepared starting by fullerene C_{60} with a modification of Hummer's synthesis using sodium nitrate, sulphuric acid and potassium permanganate as strong oxidant agents following the recipe of

reference [18]. The solution with C_{60}, sodium nitrate and sulphuric acid was stirred in an ice bath for 2 hours, while potassium permanganate was added gradually. Then the solution was further stirred for 4 hours at room temperature. After this time, the temperature was raised to 70°C and then lowered to 35°C and addition of water was made. The reaction was stopped with $H_2O_2$3% and the pH was brought to 7 with NaOH 1 M. The product was dialyzed in a dialysis bag of 2000 Da to remove the residual salts

Synthesis H_2SO_4 + HNO_3 (Synthesis B)

In the case of the synthesis with sulphuric and nitric acid, hereafter referred to as synthesis B, UFNPs were prepared starting by fullerene C_{60} and using concentrated acids H_2SO_4 and HNO_3 in a ratio 3:1. The precursors were mixed together and sonicated for 2 hours. After this time, the solution was put in an oil bath at 150°C for 24 hours. At the end, the solution was cooled down and basified to pH 7 using NaOH 15 M. The product was filtered with 0.22 μm and then dialyzed in a dialysis bag of 2000 Da to remove the residual salts.

Apparatus and data processing

Both solutions were characterized by UV-Vis absorption measurements (ABS) and photoluminescence (PL) by using quartz cuvettes with 1 cm optical path. The absorption spectra were taken with a Cary 50 spectrophotometer in the range 200 – 500 nm. The photoluminescence spectra were taken in the range 350 – 700 nm by exciting the solution with a 200-W continuous Hg(Xe) discharge lamp by a conventional 90-degree geometry. To take the spectra, apposite optical filters were used both for the excitation light and the PL signal. Fourier transform infrared spectroscopy (FT-IR) data were obtained on sample powders by a Perkin Elmer Spectrum One spectrometer (Waltham, MA, USA). In the case of XPS the surface analyses were carried in an electronic spectrometer EscalabMkII (VG Scientific Ltd., East Grinstead, UK) equipped with XPS and AES techniques. The Al Kα source was used for the photoemission and X-ray induced Auger spectroscopy, where as a LEG200 electron gun was used for the AES. The photoemission spectra were collected at 50 eV pass energy in selected area mode A3x10 with a diameter of 3 mm, whereas the Auger spectra were registered at the pass energy of 100 eV, in order to increase the signal-to-noise ratio. All experimental data were processed by using the software Avantage v.5 (Thermo Fisher Scientific, EastGrinstead, UK). Experimental C KVV spectra were smoothed at least for 11 times by moving average routine with a width of 1.2 eV. Afterwards, these spectra were differentiated by using a width of 7 data points for the determination of D parameter

Results

Characterizations of UFNPs

The PL and the absorption spectra of the two systems present some differences as reported in figure 1a. When excited at 300 nm, the PL spectrum of sample obtained from synthesis A has a maximum at 450 nm while sample obtained from synthesis B presents a red shifted peak with maximum at 500 nm and a wider shape with respect to the previous one. The absorption spectra of both solutions are reported in figure 1b. They present the typical peaks of the π-π* transitions around 200 nm and n-π* transition at 300 nm.

Materials Research Forum LLC
https://doi.org/10.21741/9781644900710-3

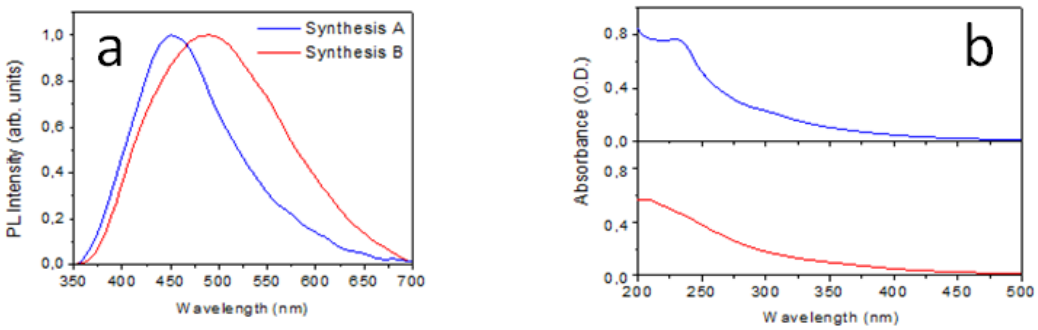

Figure 1 a) PL Intensity spectra of Synthesis A (blue line) and Synthesis B (red line);b) Absorption spectra of Synthesis A (blue line) and Synthesis B (red line)

The π-π* transitions, is due to the presence of the aromatic sp^2 domains (C=C), and the n-π* is generally attributed to the presence of C=O bonds of oxygen-containing functional groups [29]. These groups are typical of graphene oxide quantum dots (GOQDs).

In order to confirm the formation of GOQDs FT-IR spectra were acquired and shown in Figure 2.

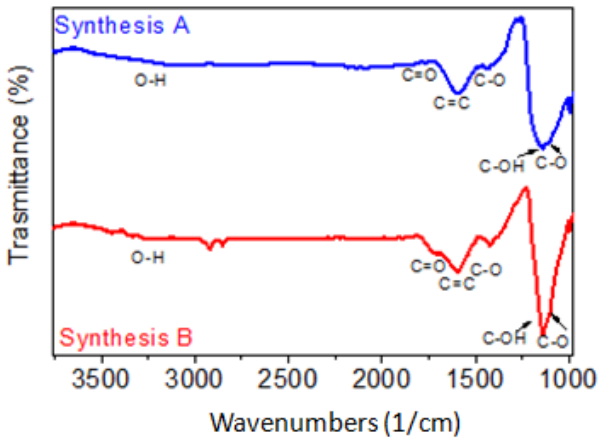

Figure 2 FT-IR spectra of Synthesis A (blue line) and Synthesis B (red line)

In both FT-IR spectra the typical peaks of graphene oxide that are related to the carboxyl, hydroxyl, and epoxy groups of GOQDs are present. In particular, the peaks at approximately 1,000 cm^{-1}, 1,150 cm^{-1}, 1,650 cm^{-1}, 1,750 cm^{-1}, and 3,350 cm^{-1} corresponding to C-O, C-OH, C=C, C=O and O-H, respectively [30].

As a general remark of the characterizations illustrated in Fig1 and Fig 2, we pointed out that, the PL of the two solutions indicates different dimension of the nanoparticles and different number of carboxylic groups. Both these factors are strongly related to the methods of synthesis and to the starting compounds [31].

It is therefore probable that a change in the number of carboxyl groups in the structure leads to a difference response in the presence of heavy metals ions.

A greater number of functional groups allows a greater interaction between GOQDs and ions.

The XPS spectra of C 1s region reported in Figs. 3(a) and 3(b) testified the prevalence of C–C bonds (main peak named as A in the Fig 3 (a) and (b)) with binding energy BE = 284.6 eV. Other two minor components of C 1s peak, attributed to C–O bonds with BE = 286.4 eV and carboxylic bonds with BE = 288.6 eV, are higher in the sample of synthesis B (Fig. 3 (b)).

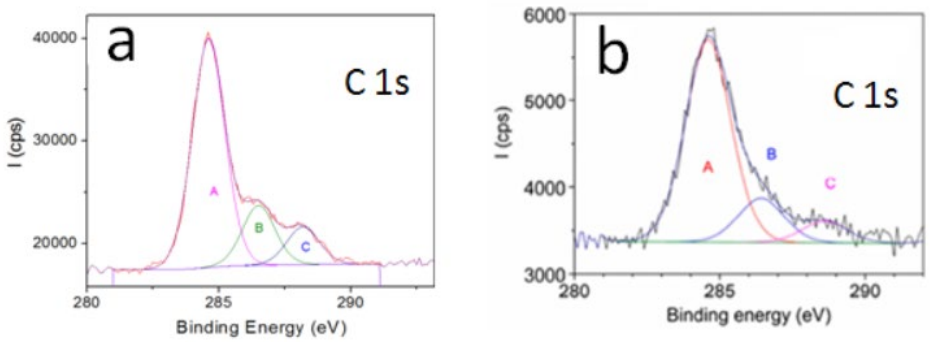

Figure 3 XPS spectra of carbon related to the samples of synthesis A (a) and synthesis B (b).

From the comparison of Auger spectra of C KVV region (Figure 4) acquired by using X-rays and electron beam (see Figure 4 (a)), were determined the values of D parameter equal to 12.7 and 20.9 eV, respectively. This change of the D parameter from the diamond-like value obtained with X-rays to graphitic one (electron beam) indicates that the main configuration of C–C bonds in the sample of synthesis A corresponds to graphene [32]. In the sample of synthesis B, the D parameter obtained from X-rays excited C KVV spectrum (Fig. 4(b)) is higher (15.1 eV) due to the higher amount of C-O and carboxylic bonds.

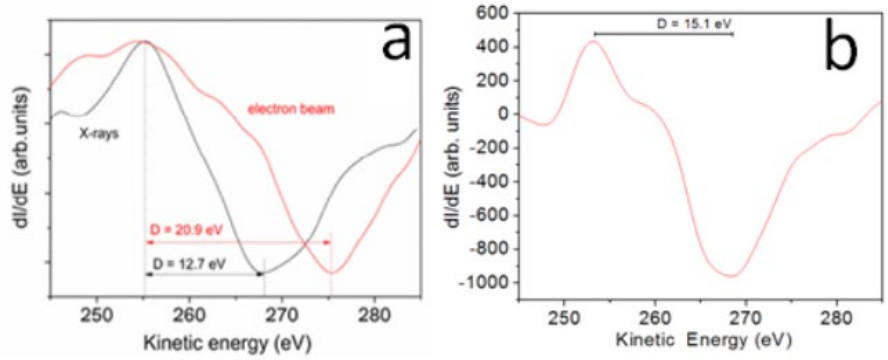

Figure 4 Auger spectra of C KVV region of the samples of synthesis A (a) and synthesis B (b).

Excitation spectra of UFNPs

GOQDs have localized sp2 carbon subdomains having specific absorption energy levels with similar DOS (density of states) as reported by many works [33,34]. These energy states were studied by different authors [33,34] and recently their presence was confirmed by a red-blue-red (RBR) shift of the PL spectra using different excitation wavelengths [35,36].

In figure 5 the emission spectra at various excitation wavelengths of the two systems are reported. For synthesis A (Figure 5(a)), the emission spectra are reported in the excitation range

270 – 360 nm, while, for synthesis B are reported in the range 280 – 400 nm (Figure 5(b)). As it is possible to see from the graph, in the synthesis B case, the maximum of photoluminescence spectrum has an RBR shift [35,36]. Specifically, a redshift is present in the excitation wavelength range 280–290 nm, subsequently a blueshift in 300–340 nm, and a redshift in the range 340–500 nm. In the case of synthesis A, this shift is no present.

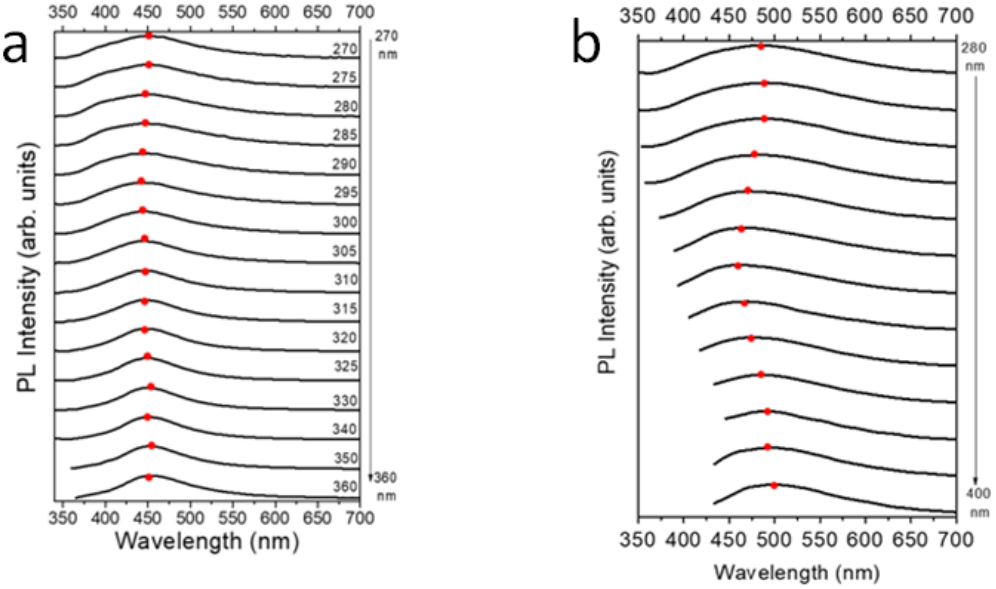

Figure 5 a) Emission spectra of synthesis A in the excitation range 270 – 360 nm; b) Emission spectra of synthesis B in the excitation range 280 – 400 nm

Called intrinsic state the state formed by localized sp2 carbon subdomains, and extrinsic states the state due to the presence of the oxygen-containing groups [35,36], the difference in the emission spectra at various excitation can be related to the number variation of intrinsic and extrinsic states. The RBR shift is present when the intrinsic and extrinsic states are in greater numbers, in fact, for synthesis B the number of oxygen-containing groups is greater than the synthesis A, and this is due to the synthesis method. In fact, a different synthesis method causes a variation of defective groups, thus a variation in the number of intrinsic and extrinsic groups. For this reason, the RBR shift is present for the synthesis B.

Heavy metal sensitivity

We measured the optical response of the both synthesized systems to test the presence of heavy metal ions in water. The ratio of the fluorescence intensity of the two UFNPs syntheses, with and without of metal ions in the solution is reported in figure 6 for several metal ions.

In order to characterize the system response in the presence of these ions at the concentration of 100 µM, a drop of 30 µl of concentrated salt solution was added to 3 ml of UFNPs solution. The pH of the solution was measured immediately before and after each measurement and it was 7. The investigated ions were: Co(II), Cu(II), Cd(II), Pb(II), Ni(II), Na(I), As(III), and As(V).

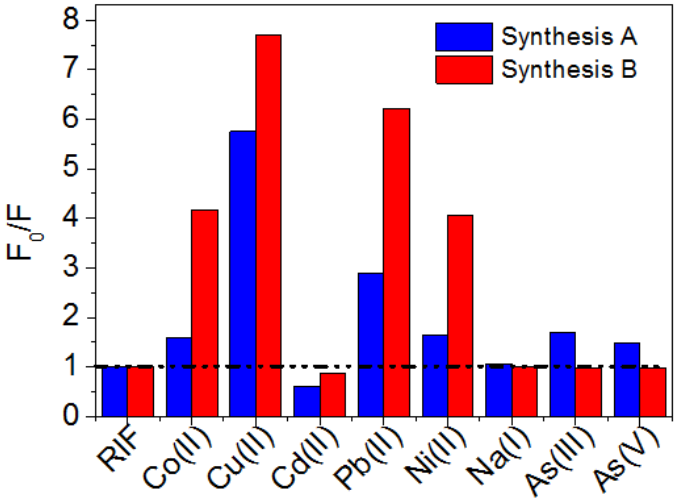

Figure 6 Response in the presence of different heavy metal ions at 100 µM concentration for Synthesis A (blue bar) and Synthesis B (red bar)

As stated in our previous works [27,28,37] we reported different studies about the interaction between UFNPs and heavy metal ions. Due to an aggregation process, the interaction of heavy metal ions and UFNPs can cause the formation of a stable complex [37,38]. In fact, metal ions can bind more quantum dots together thanks to the presence of the oxygen-containing groups at the edge and at the surface of the UFNPs structure [38-40]. This aggregation is responsible for a change of the PL intensity.

The binding with a specific ion depends by the affinity between the ion and the UFNPs. This mechanism plays an important role in the Photoinduced Electron Transfer (PET) in the UFNPs and therefore, the presence of some ions causes a quenching or an enhancement of the PL signal. The UFNPs synthesized with Hummer method shows a fluorescence quenching and an increase of absorption in the short wavelength range of absorbance spectrum (not shown here, see reference [27]) in the presence of Cu(II) and Pb(II) ions, as we reported recently [27]. This has been explained with the interaction of metal ions with the carboxyl groups located at the edges of UFNPs, possibly promoting an edge-to-edge aggregation. In the case of the arsenic ions, the aggregation could be face-to-face [40]. Both types of aggregation allow the chelation of metal ions, with a consequence of PL quenching effect. In the case of cadmium ions, the PL enhanced could be due to the Chelation-Enhanced Fluorescence (CHEF) mechanism [40,41], Cd(II) ions might coordinate with the basal surface of the carbon layers trough cation-π interaction [41-43] using the oxygen lone pair electrons of the carbonyl and epoxy groups by immobilizing the lone pair electrons, Cd(II) cation increases the recombination rate and the fluorescence intensity of UFNPs.

In the figure 5 both syntheses have a similar behaviour in the presence of the different ions, but in the case of synthesis B, the system is more sensitive. This is probably due to a greater oxidation degree of the system, in fact, FT-IR spectra (Figure 2), XPS (Figure 3) and Auger spectroscopy (Figure 4) confirm the greater presence of carboxylic groups. Or probably, it is due the different synthesis method, without potassium permanganate. In fact, the use of potassium permanganate can limit the response of the system, due to possible interaction between Mn(II) ions and quantum dots. Not using the permanganate in the synthesis could allow to obtain a more sensitive system.

An important aspect about the response of the two systems in presence of the arsenic ions is reported: As(III) and As(V) not affect the optical signal in the synthesis B, while the both As

ions increase the PL emission of the synthesis A. Such a behaviour is probably related to the oxidative groups that are mainly at the edge of the GOQDs, while the arsenic is known to bind preferentially with the surface of the carbon nanosheets, rather than the edge [40,41]. Thanks to the different response in the case of arsenic ions by using both UFNPs solutions it could be possible to detect selectively these ions in water.

Conclusions

A new synthesis of UFNPs starting from C_{60} fullerene was studied by using only two strong acid as oxidant agents. The obtained material was studied and tested to detect different heavy metal ions in water, and the results were compared with our previous synthesis of UFNPs by a modification of Hummer method. A different oxidation degree of carbon is confirmed by FT-IR analysis and XPS. The different structure obtained have different number of extrinsic and intrinsic states and for this reason there is a different response in the emission spectra at various excitation wavelength. The second system is more sensitive to the presence of heavy metal ions, but very interesting in the different response in the presence of As(III) and As(V). In fact, in the case of the second synthesis, the system doesn't respond to the presence of these ions on the contrary of synthesis A. Further studies are necessary to understand this behavior, but these two systems can be used to detect the presence of arsenic in water.

Acknowledgments

This research was funded by Regione Lazio, through Progetto di ricerca 85-2017-15125, according to L.R.13/08 and by the University of Rome Tor Vergata in the framework of “GHOST” project, within “Mission Sustainability" program (D.R. 2817/2016), grant number (CUP): E86C18000450005.

References

[1] X. T. Zheng, A. Ananthanarayanan, K. Q. Luo, and P. Chen, “Glowing Graphene Quantum Dots and Carbon Dots : Properties , Syntheses , and Biological Applications” Small, vol. 11, no. 14, pp. 1620–1636, 2015. https://doi.org/10.1002/smll.201402648

[2] L. Fan, Y. Hu, X. Wang, L. Zhang, F. Li, D. Han, L. Zhenggang, Z. Qixian, Z. Wang and L. Niu, “Fluorescence resonance energy transfer quenching at the surface of graphene quantum dots for ultrasensitive detection of TNT” Talanta, vol. 101, pp. 192–197, 2012. https://doi.org/10.1016/j.talanta.2012.08.048

[3] M. K. Kumawat, M. Thakur, R. B. Gurung, and R. Srivastava, “Graphene Quantum Dots for Cell Proliferation, Nucleus Imaging, and Photoluminescent Sensing Applications” Sci. Rep., vol. 7, no. 1, pp. 1–16, 2017. https://doi.org/10.1038/s41598-017-16025-w

[4] F. Wang, Z. Gu, W. Lei, W. Wang, X. Xia, and Q. Hao, “Graphene quantum dots as a fluorescent sensing platform for highly efficient detection of copper (II) ions” Sensors Actuators B. Chem., vol. 190, pp. 516–522, 2014. https://doi.org/10.1016/j.snb.2013.09.009

[5] E. Zor, E. Morales-Narváez, A. Zamora-Gálvez, H. Bingol, M. Ersoz, and A. Merkoçi, “Graphene quantum dots-based photoluminescent sensor: A multifunctional composite for pesticide detection” ACS Appl. Mater. Interfaces, vol. 7, pp. 20272–20279, 2015. https://doi.org/10.1021/acsami.5b05838

[6] T. Wu, H. Shen, L. Sun, B. Cheng, B. Liu, and J. Shen, “Nitrogen and boron doped monolayer graphene by chemical vapor deposition using polystyrene, urea and boric acid” New J. Chem., vol. 36, no. 6, pp. 1385–1391, 2012. https://doi.org/10.1039/c2nj40068e

[7] Y. Dong, J. Shao, C. Chen, H. Li, R. Wang, Y. Chi, X. Lin and G. Chen, "Blue luminescent graphene quantum dots and graphene oxide prepared by tuning the carbonization degree of citric acid" Carbon N. Y., vol. 50, pp. 4738–4743, 2012. https://doi.org/10.1016/j.carbon.2012.06.002

[8] I. Shtepliuk, N. M. Caffrey, T. Iakimov, V. Khranovskyy, I. A. Abrikosov, and R. Yakimova, "On the interaction of toxic Heavy Metals (Cd, Hg, Pb) with graphene quantum dots and infinite graphene" Sci. Rep., vol. 7, no. 1, p. 3934, 2017. https://doi.org/10.1038/s41598-017-04339-8

[9] R. Sitko, E. Turek, B. Zawisa, E. Malicka, E. Talik, J. Heimann, A. Gagor, B. Feist and R. Wrzalik, "Adsorption of divalent metal ions from aqueous solutions using graphene oxide" Dalt. Trans., vol. 42, no. 16, p. 5682, 2013. https://doi.org/10.1039/c3dt33097d

[10] Jian Ju and W. Chen, "Graphene Quantum Dots as a Fluorescence Probes for Sensing Metal Ions: Synthesis and Applications" Curr. Org. Chem., vol. 19, pp. 1150–1162, 2015. https://doi.org/10.2174/1385272819666150318222547

[11] D. Wang, L. Wang, X. Dong, Z. Shi, and J. Jin, "Chemically tailoring graphene oxides into fluorescent nanosheets for Fe3+ ion detection" Carbon N. Y., vol. 50, no. 6, pp. 2147–2154, 2012. https://doi.org/10.1016/j.carbon.2012.01.021

[12] H. Chakraborti, S. Sinha, S. Ghosh, and S. Kalyan, "Interfacing water soluble nanomaterials with fluorescence chemosensing : Graphene quantum dot to detect Hg2+ in 100 % aqueous solution" Mater. Lett., vol. 97, pp. 78–80, 2013. https://doi.org/10.1016/j.matlet.2013.01.094

[13] Z. Li, Y. Wang, Y. Ni, and S. Kokot, "A rapid and label-free dual detection of Hg (II) and cysteine with the use of fluorescence switching of graphene quantum dots" Sensors Actuators B. Chem., vol. 207, pp. 490–497, 2015. https://doi.org/10.1016/j.snb.2014.10.071

[14] H. Huang, L. Liao, X. Xu, M. Zou, F. Liu, and N. Li, "The electron-transfer based interaction between transition metal ions and photoluminescent graphene quantum dots (GQDs): A platform for metal ion sensing" Talanta, vol. 117, pp. 152–157, 2013. https://doi.org/10.1016/j.talanta.2013.08.055

[15] S. Huang, H. Qiu, F. Zhu, S. Lu, and Q. Xiao, "Graphene quantum dots as on-off-on fluorescent probes for chromium (VI) and ascorbic acid" Microchim. Acta, vol. 182, pp. 1723–1731, 2015. https://doi.org/10.1007/s00604-015-1508-6

[16] X. Liu, W. Gao, and X. Zhou, "Pristine graphene quantum dots for detection of copper ions" J. Mater. Res., vol. 29, no. 13, pp. 1401–1407, 2014. https://doi.org/10.1557/jmr.2014.145

[17] R. Xie, Z. Wang, W. Zhou, Y. Liu, L. Fan, Y. Li, and X. Li, "Graphene quantum dots as smart probes for biosensing" Anal. Methods, vol. 8, no. 20, pp. 4001–4006, 2016. https://doi.org/10.1039/C6AY00289G

[18] C. K. Chua, Z. Sofer, P. Simek, O. Jankovsky, K. Klimova, S. Bakardjieva and M. Pumera , "Synthesis of strongly fluorescent graphene quantum dots by cage-opening buckminsterfullerene" ACS Nano, vol. 9, no. 3, pp. 2548–2555, 2015. https://doi.org/10.1021/nn505639q

[19] X. Tan, Y. Li, X. Li, S. Zhou, L. Fan, and S. Yang, "Electrochemical synthesis of small-sized red fluorescent graphene quantum dots as a bioimaging platform" Chem. Commun., vol. 51, no. 13, pp. 2544–2546, 2015. https://doi.org/10.1039/C4CC09332A

[20] K. Li, W. Liu, Y. Ni, D. Li, D. Lin, Z. Su and G. Wei, “Technical synthesis and biomedical applications of graphene quantum dots” J. Mater. Chem. B, vol. 5, no. 25, pp. 4811–4826, 2017. https://doi.org/10.1039/C7TB01073G

[21] L. L. Li, J. Ji, R. Fei, C. Z. Wang, Q. Lu, J. R. Zhang, and J. J. Zhu, “A Facile Microwave Avenue to Electrochemiluminescent Two-Color Graphene Quantum Dots” Adv. Funct. Mater., vol. 22, no. 14, pp. 2971–2979, 2012. https://doi.org/10.1002/adfm.201200166

[22] F. Liu, M. H. Jang, H. D. Ha, J. H. Kim, Y. H. Cho, and T. S. Seo, “Facile synthetic method for pristine graphene quantum dots and graphene oxide quantum dots: Origin of blue and green luminescence” Adv. Mater., vol. 25, no. 27, pp. 3657–3662, 2013. https://doi.org/10.1002/adma.201300233

[23] L. Staudenmaier, “Darstellung der Graphitslure” Ger. Chem. Soc., vol. 31, no. 2, pp. 1481–1487, 1898. https://doi.org/10.1002/cber.18980310237

[24] H. P. Boehm, A. Clauss, G. O. Fischer, and U. Hofmann, “Dünnste kohlenstoff-folien” Zeitschrift fur Naturforsch. - Sect. B J. Chem. Sci., vol. 17, no. 3, pp. 150–153, 1962. https://doi.org/10.1515/znb-1962-0302

[25] W. S. Hummers and R. E. Offeman, “Preparation of Graphitic Oxide” J. Am. Chem. Soc., vol. 80, no. 6, p. 1339, 1958. https://doi.org/10.1021/ja01539a017

[26] C. Botas P. Álvarez, P. Blanco, M. Granda, C. Blanco, R. Santamaría, and R. Menéndez, , “Graphene materials with different structures prepared from the same graphite by the Hummers and Brodie methods” Carbon N. Y., vol. 65, pp. 156–164, 2013. https://doi.org/10.1016/j.carbon.2013.08.009

[27] E. Ciotta, P. Prosposito, P. Tagliatesta, C. Lorecchio, L. Stella, S. Kaciulis, P. Soltani, E. Placidi and R. Pizzoferrato, “Discriminating between different heavy metal ions with fullerene-derived nanoparticles” Sensors (Switzerland), vol. 18, no. 5, pp. 1–15, 2018. https://doi.org/10.3390/s18051496

[28] E. Ciotta, S. Paoloni, M. Richetta, P. Prosposito, P. Tagliatesta, C. Lorecchio, I. Venditti, I. Fratoddi, S. Casciardi and R. Pizzoferrato, “Sensitivity to Heavy-Metal Ions of Unfolded Fullerene Quantum Dots” Sensors, vol. 17, p. 2614, 2017. https://doi.org/10.3390/s17112614

[29] A. V Naumov, Optical Properties of Graphene Oxide, in Graphene Oxide: Fundamentals and Applications. Chichester, UK: John Wiley & Sons, Ltd, 2016. https://doi.org/10.1002/9781119069447.ch5

[30] L. Yun and Z. Kyusik, “Graphene oxide-modified ZnO particles: synthesis, characterization , and antibacterial properties” Int. J. Nanomedicine, vol. 10, pp. 79–92, 2015. https://doi.org/10.2147/IJN.S88319

[31] S. J. Bradley, R. Kroon, G. Laufersky, M. Röding, R.V. Goreham, T. Gschneidtner, and T. Nann., “Heterogeneity in the fluorescence of graphene and graphene oxide quantum dots” Microchim. Acta, vol. 184, no. 3, pp. 871–878, 2017. https://doi.org/10.1007/s00604-017-2075-9

[32] S. Kaciulis, A. Mezzi, P. Calvani and D.M. Trucchi, "Electron spectroscopy of the main allotropes of carbon", Surf. Interface Anal., vol. 46, pp. 966-969, 2014. https://doi.org/10.1002/sia.5382

[33] P. Huang, J.J. Shi, M. Zhang, X. H. Jiang, H. X. Zhong, Y.M. Ding and J. Lu, "Anomalous Light Emission and Wide Photoluminescence Spectra in Graphene Quantum Dot: Quantum Confinement from Edge Microstructure" J. Phys. Chem. Lett., vol. 7, no. 15, pp. 2888–2892, 2016. https://doi.org/10.1021/acs.jpclett.6b01309

[34] Y. Li, H. Shu, S. Wang, and J. Wang, "Electronic and optical properties of graphene quantum dots: The role of many-body effects" J. Phys. Chem. C, vol. 119, no. 9, pp. 4983–4989, 2015. https://doi.org/10.1021/jp506969r

[35] M. H. Jang, S. H. Song, H. D. Ha, T. S. Seo, S. Jeon, and Y. H. Cho, "Origin of extraordinary luminescence shift in graphene quantum dots with varying excitation energyAn experimental evidence of localized sp2 carbon subdomain" Carbon N. Y., vol. 118, pp. 524–530, 2017. https://doi.org/10.1016/j.carbon.2017.03.060

[36] C. T. Chien, S. Li, W.J. Lai, Y. Yeh, H. A. Chen, I. S. Chen, and M. Chen, "Tunable photoluminescence from graphene oxide" Angew. Chemie - Int. Ed., vol. 51, no. 27, pp. 6662–6666, 2012. https://doi.org/10.1002/anie.201200474

[37] E. Ciotta, P. Prosposito, and R. Pizzoferrato, "Positive curvature in Stern-Volmer plot described by a generalized model for static quenching" J. Lumin., vol. 206, pp. 518–522, 2019. https://doi.org/10.1016/j.jlumin.2018.10.106

[38] H. Huang, L. Liao, X. Xu, M. Zou, F. Liu, and N. Li, "The electron-transfer based interaction between transition metal ions and photoluminescent graphene quantum dots (GQDs): A platform for metal ion sensing" Talanta, vol. 117, pp. 152–157, 2013. https://doi.org/10.1016/j.talanta.2013.08.055

[39] L. Wu, L. Liu, B. Gao, R. Muñoz-Carpena, M. Zhang, H. Chen, and H. Wang,, "Aggregation kinetics of graphene oxides in aqueous solutions: Experiments, mechanisms, and modeling" Langmuir, vol. 29, no. 49, pp. 15174–15181, 2013. https://doi.org/10.1021/la404134x

[40] S. T. Yang , Y. Chang, H. Wang, G. Liu, S. Chen, Y. Wang, and A. Cao, A., "Folding/aggregation of graphene oxide and its application in Cu2+ removal" J. Colloid Interface Sci., vol. 351, no. 1, pp. 122–127, 2010. https://doi.org/10.1016/j.jcis.2010.07.042

[41] X. Yang, L. Xia, and S. Song, "Arsenic Adsorption From Water Using Graphene-Based Materials As Adsorbents: a Critical Review" Surf. Rev. Lett., vol. 24, no. 01, p. 1730001, 2017. https://doi.org/10.1142/S0218625X17300015

[42] A. T. Afaneh and G. Schreckenbach, "Fluorescence Enhancement/Quenching Based on Metal Orbital Control: Computational Studies of a 6-Thienyllumazine-Based Mercury Sensor" J. Phys. Chem. A, vol. 119, no. 29, pp. 8106–8116, 2015. https://doi.org/10.1021/acs.jpca.5b04691

[43] I. Shtepliuk, V. Khranovskyy, and R. Yakimova, "Insights into the origin of the excited transitions in graphene quantum dots interacting with heavy metals in different media" Phys. Chem. Chem. Phys., vol. 19, no. 45, pp. 30445–30463, 2017. https://doi.org/10.1039/C7CP04711H